

# Investigations on the surface modification of ZnO nanoparticle photocatalyst by depositing Pd

Jing Liqiang<sup>a,b</sup>, Wang Baiqi<sup>b</sup>, Xin Baifu<sup>a</sup>, Li Shudan<sup>a</sup>, Shi Keying<sup>a</sup>, Cai Weimin<sup>b</sup>,  
Fu Honggang<sup>a,\*</sup>

<sup>a</sup>*School of Chemistry and Material Sciences, The Key Laboratory of Physical Chemistry, Heilongjiang University, Number 74, Xuefu Road, Nangang District, Harbin city, Heilongjiang Province 150080, China*

<sup>b</sup>*Department of Environmental Sciences and Engineering, Harbin Institute of Technology, Harbin 150001, China*

Received 7 June 2004; received in revised form 4 August 2004; accepted 7 August 2004

## Abstract

In this paper, ZnO nanoparticle photocatalysts were modified by depositing Pd on their surfaces with a photoreduction method. We mainly investigated the modification mechanisms as well as the effects on the photocatalytic activity of ZnO nanoparticles of deposited Pd by means of XPS and SPS (Surface Photovoltage Spectroscopy), and the effects of Pd content on SPS responses were also discussed from the point of the electronic energy level. The results showed that the content of crystal lattice oxygen on the surface of ZnO nanoparticle decreased after an appropriate amount of Pd was deposited, while that of adsorbed oxygen increased, indicating that Pd was mainly deposited on the crystal lattice oxygen. At the same time, the intensity of SPS responses of ZnO nanoparticles remarkably decreased. In addition, the activity of ZnO nanoparticles could be greatly improved by depositing an appropriate amount of Pd in the gas phase photocatalytic oxidation of *n*-C<sub>7</sub>H<sub>16</sub>. Thus, it could be concluded that the increase in surface content of adsorbed oxygen could facilitate the photocatalytic reaction, and there were close relationships between the SPS response and photocatalytic activity, i.e. the weaker the SPS response, the higher the photocatalytic activity, of Pd-deposited ZnO nanoparticles.

© 2004 Elsevier Inc. All rights reserved.

**Keywords:** ZnO; Nanoparticle; Surface modification; Pd; Photocatalysis

## 1. Introduction

Recently, nanosized semiconductor materials have attracted increasing attention to a wide range of possible applications such as solar energy cells as photoelectric energy conversion materials [1–5] and water or air purification as friendly environmental photocatalyst [6–8]. The basis and more significant applications of semiconductor photocatalytic oxidation have been extensively documented in the last 20 years [6–12]. One of the main problems associated with feasibility and viability of semiconductor photocatalytic oxidation is represented by a high tendency of photoinduced hole–

electron pairs to recombine, leading to lower activity of semiconductor photocatalysts. The use of electronic scavengers like adsorbed O<sub>2</sub> is a good alternative to overcome this problem. Moreover, some studies have demonstrated that the existence of noble metal atomic clusters such as Pt [13,14], Pd [15] and Ag [4,16,17] on the surfaces of semiconductor particles could improve the activity by inhibiting the recombination of photoinduced electron–hole pairs [18,19]. However, few papers were involved with SPS technique. Among many semiconductor materials, ZnO is one of potential materials in solar energy conversion and photocatalytic field due to its photochemical properties similar to TiO<sub>2</sub> [20]. However, up to date, semiconductor photocatalysts, other than TiO<sub>2</sub>, are much less studied. Furthermore, ZnO nanoparticle is very cheap and easy to be prepared.

\*Corresponding author. Fax: 86-451-8660-7792.

E-mail address: [jilqiang@sohu.com](mailto:jilqiang@sohu.com) (F. Honggang).

In this paper, the modification mechanisms and the effects on the photocatalytic activity and SPS response of ZnO nanoparticles of deposited Pd were mainly investigated by means of XPS and SPS techniques. The results showed that there were certain relations between the SPS response and photocatalytic activity of Pd deposited ZnO nanoparticles, which was because the SPS response and photocatalytic activity both were closely related to the photoinduced charge carriers. It should be of significance in semiconductor environmental photocatalysis by providing solid basis in the theory to prepare new semiconductor photocatalyst with higher activity.

## 2. Experimental

All substances were of analytical grade and used without further purification. Deionized water was used to prepare all solutions.

### 2.1. Preparation of ZnO nanoparticles modified by depositing Pd

ZnO nanoparticles were prepared by calcining the precursor, zinc carbonate hydroxide,  $\text{Zn}_5(\text{CO}_3)_2(\text{OH})_6$ , at 320 °C which was described in previous papers in detail [21,22], and also were modified by depositing Pd on their surfaces using photoreduction method [23,24] as following. Firstly,  $7.06 \times 10^{-3}$  M of  $\text{PdCl}_2$  solution containing 1.25%  $\text{CH}_3\text{COOH}$  and 1.25%  $\text{CH}_3\text{COOH}$  solution were prepared. The  $\text{CH}_3\text{COOH}$  solution was regarded as a sacrificial organic substance to capture photoinduced holes so as to improve the efficiency of utilizing photoinduced electrons. Then, 20 mL of a mixture consisting of needed amount of  $\text{PdCl}_2$  solution and  $\text{CH}_3\text{COOH}$  solution was added to a 100 mL beaker containing 0.5 g of ZnO nanoparticles, which was ultrasonicated for 10 min. Subsequently, the mixture was transferred into a cylindrical quartz tube photoreactor of 300 mL placed horizontally with two mouths at its two ends. The photoreactor was blown through ultrapure  $\text{N}_2$  gas for 5 min in order to drive out  $\text{O}_2$  gas within the reactor after being sealed. Finally, the photoreactor was submitted to a UV irradiation treatment by a 400 W high-pressure mercury lamp ( $\lambda_{\text{max}} = 365$  nm) for 6 h. Thus, ZnO nanoparticles modified by Pd with different desired content could be obtained by centrifugating and washing with water and drying at 80 °C.

In addition, the concentration of Pd in the mixture treated by UV light for 6 h was tested by an inductively coupled plasma-atomic emission spectrometry (a PE ICP-AES/1000), demonstrating that the deposit rate of Pd was more than 90% in our experiments.

### 2.2. Characterization of the samples

The samples were analyzed by XRD using a Rigaku D/MAX-rA powder diffractometer with a nickel-filtered  $\text{CuK}\alpha$  radiation source. The crystal phase and crystallite size were determined from the X-ray diffraction patterns. The samples were examined with a JEOL-1200EX TEM. The size and morphology were measured by TEM micrographs.

SPS measurement of the samples was carried out with a home-built apparatus that had been described elsewhere [25–28]. It was performed by a photovoltage cell, mainly consisting of two ITO quartz glass electrodes. For a semiconductor powder experiment, the powder sample is sandwiched between two ITO quartz glass electrodes. The surface composition of the samples was examined by a VG ESCALAB MKII X-ray source. The pressure was maintained at  $6.3 \times 10^{-5}$  Pa. The binding energies were calibrated with respect to the signal for adventitious carbon (binding energy = 284.6 eV). Quantitative analysis was carried out using the sensitivity factors supplied by the instrument.

### 2.3. Evaluation of photocatalytic activity of the samples

The light source used in this experiment was a 400 W high-pressure mercury lamp ( $\lambda_{\text{max}} = 365$  nm). The UV light was transmitted to the specimen through a quartz tube placed between the UV lamp and the photoreactor to adsorb the heat and transmit UV light. The reactor used was a 300 mL cylindrical quartz tube. 0.1 g of the photocatalyst was spread uniformly over the internal surface of the reactor as a thin layer by carefully shaking. After this, the reactor was vacuum-packed and 1.2 mL of  $n\text{-C}_7\text{H}_{16}$  and 63 mL of oxygen were injected into the reactor through a sample port. Then, the ultrapure nitrogen (99.9999%) was mixed with the reactant in the reactor to a little higher than one atmospheric pressure. Thus, the reactants were  $n\text{-C}_7\text{H}_{16}$  (4%, balance nitrogen) and oxygen (21%, balance nitrogen). When the adsorption reached equilibrium, as measured by gas chromatogram (GC), the reaction started by turning on the lamp. Subsequently, the concentration of  $n\text{-C}_7\text{H}_{16}$  in the reactor, obtained by a gastight syringe from the sample port, was measured every 30 min by a Varian 3700 GC equipped with a flame ionization detector and a SE-54 quartz capillary column at 60 °C. The reaction ended by turning off the lamp [29,30].

## 3. Results and discussion

### 3.1. Measurements of XRD and TEM

Fig. 1 showed the XRD patterns of pure and 0.5 wt% Pd-deposited ZnO nanoparticles. The results

demonstrated that pure and Pd deposited ZnO nanoparticles all were with wurtzite structure attached to hexagonal crystal system, and their average crystallite sizes, evaluated by the Scherrer formula [21,22], were about 13 nm, indicating that the crystallinity of the samples did not change a little. The content of deposited Pd might be too less to determine its existence, which possibly indicated that Pd was dispersed uniformly onto the surfaces of ZnO nanoparticles.

In addition, from TEM micrographs, shown in Fig. 2, of pure (A) and 0.5 wt% Pd deposited (B) ZnO nanoparticles, it could be found that noble metal Pd exhibited much black compared with ZnO particle, and formed clusters other than an evenly covering layer. The average size of pure ZnO nanoparticles was 13 nm, while that of Pd deposited ZnO nanoparticles was 25 nm, demonstrating that ZnO nanoparticles easily aggregated during the process of the photoreduction. Moreover, the particle size is the same as the crystallite size for pure ZnO nanoparticles, which indicated that pure ZnO nanoparticles could easily be dispersed.

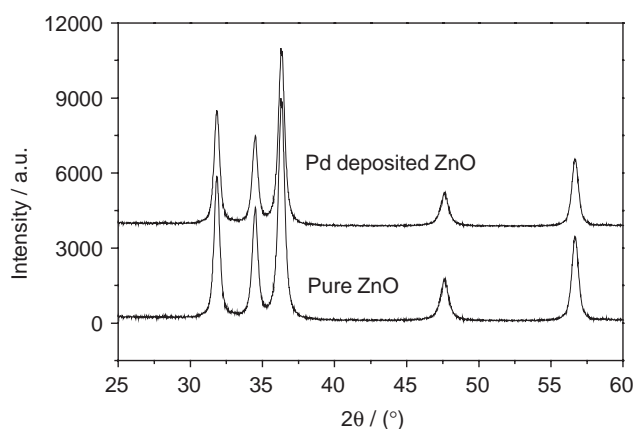


Fig. 1. The XRD patterns of pure and Pd deposited ZnO nanoparticles.

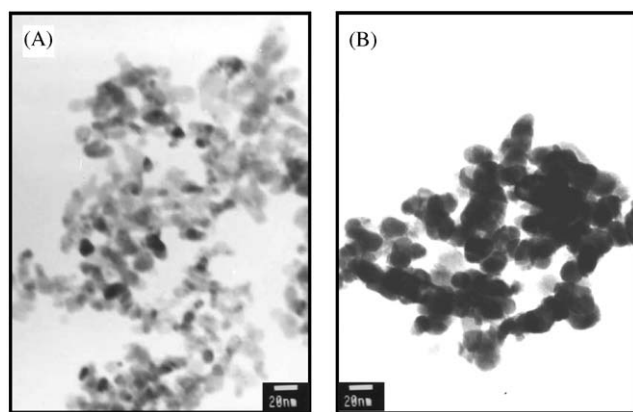


Fig. 2. TEM micrographs of pure (A) and Pd deposited (B) ZnO nanoparticles.

### 3.2. Measurement of XPS

The pure and 0.5 wt% Pd deposited ZnO nanoparticles were examined with XPS technique. Fig. 3 showed the XPS spectrum of Pd<sub>3d</sub>, it could be seen that the XPS signal was weak due to its low content, and the binding energy position of the Pd<sub>3d</sub> XPS peak was at about 335.5 eV. In general, the binding energy of Pd<sub>(3d5)<sup>2+</sup> is more than 336.0 eV according to the binding energy handbook of the XPS instrument. Thus, it could be concluded that the Pd element mainly existed as atomic form with 0 valence, combined with TEM results, indicating that the Pd atomic clusters were formed on the surface of ZnO nanoparticles.</sub>

Fig. 4 showed the XPS spectra of Zn<sub>2p</sub> (A) and O<sub>1s</sub> (B). As seen from Fig. 4, the position of XPS peak of Zn<sub>2p</sub> did not change much after Pd was deposited, while that of O<sub>1s</sub> changed remarkably. The XPS peak of Zn<sub>2p</sub> was sharp, while that of O<sub>1s</sub> was asymmetric. Thus, we could conclude that there were mainly Zn<sup>2+</sup> and not less than two kinds of oxygen species. The XPS spectra of O<sub>1s</sub> should be divided into three kinds of chemical states according to the binding energy range from 528 to 534 eV, attributed to crystal lattice oxygen, chemically adsorbed oxygen and physically adsorbed oxygen with increasing binding energy, respectively [23,24]. For a careful XPS analysis, Fig. 5 showed the O<sub>1s</sub> XPS spectrum of pure ZnO nanoparticles to be fitted to three kinds of oxygen species by Gaussian rule, taken as an instance. In addition, the relatively quantitative analysis can be performed by utilizing the XPS peak area of different elements and their own sensitivity factor according to the following equation:  $n(E1)/n(E2) = [A(E1)/S(E1)]/[A(E2)/S(E2)]$ , where  $n$  is the atomic number,  $E$  is a element,  $S$  is elemental sensitivity factor. Thus, some important XPS data could be obtained.

Table 1 showed the XPS data of Zn<sub>2p</sub> and O<sub>1s</sub>, mainly including the binding energy of Zn and different

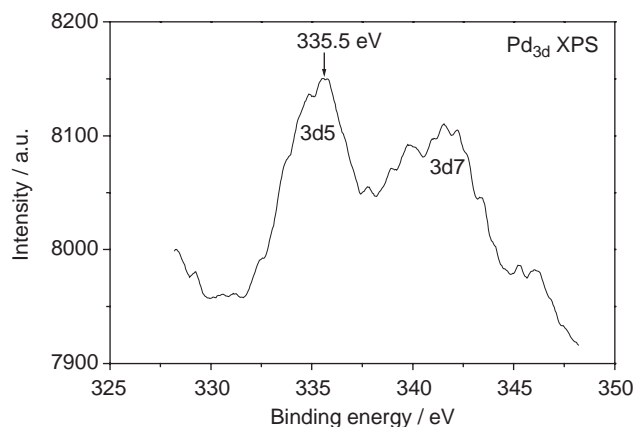


Fig. 3. XPS spectrum of Pd<sub>3d</sub> on the surfaces of Pd deposited ZnO nanoparticles.

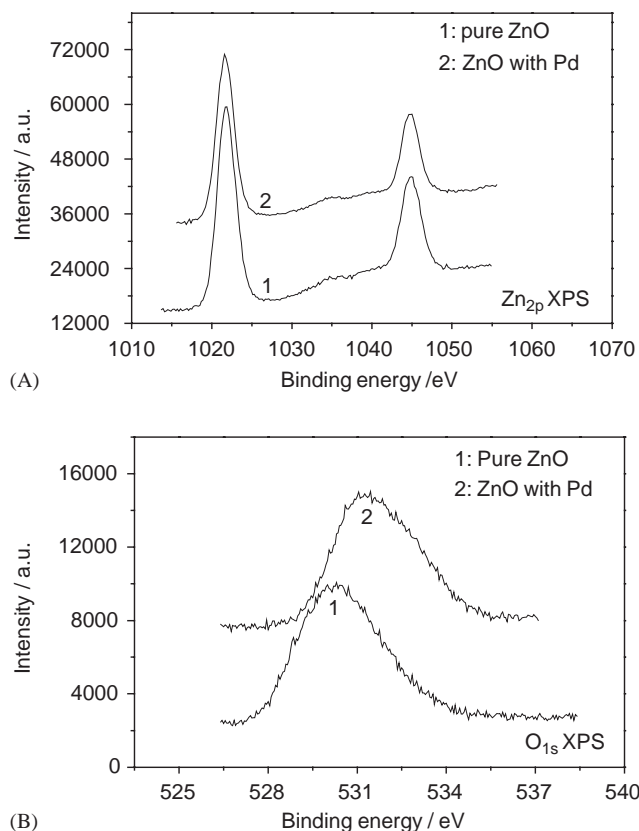


Fig. 4. XPS spectra of  $Zn_{2p}$  (A) and  $O_{1s}$  (B) on the surfaces of pure and Pd deposited ZnO.

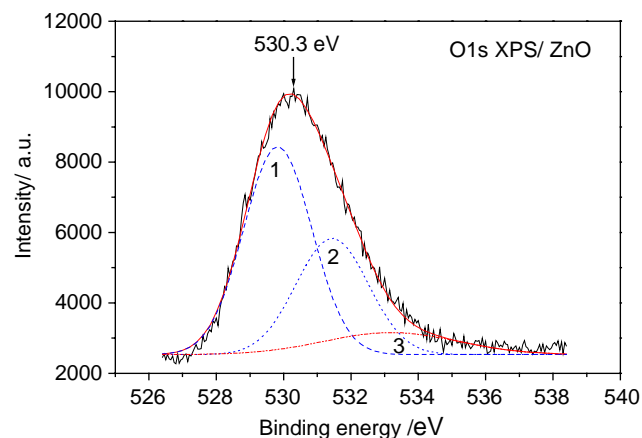


Fig. 5. The  $O_{1s}$  XPS spectrum of pure ZnO nanoparticles fitted to three kinds of oxygen species.

chemical state O and atomic number ratio of Zn/O. It could be seen that the atomic number ratio of Zn/O (crystal lattice) increased after Pd was deposited, while that of Zn/O (total) decreased a little, indicating that the content of crystal lattice oxygen decreased, while that of adsorbed oxygen increased, although that of total oxygen increased a little. These demonstrated that Pd

was mainly deposited on the crystal lattice oxygen, possibly being responsible for the forming of noble metal atomic clusters other than an evenly covering layer. Moreover, according to the principle of photocatalysis [7–9], it was the most effective for noble metal cations like  $Pd^{2+}$  as the receptors of photoinduced electron to be adsorbed on the crystal lattice oxygen among three kinds of oxygen species during the process of photoreduction. In addition, the deposit of noble metal like Pd can enhance the ability of ZnO to adsorb  $O_2$  [31], which made the position of  $O_{1s}$  XPS peak shift to higher binding energy (seeing Fig. 4B).

During the process of gas phase photocatalytic reaction, the  $O_2$  adsorbed on semiconductor photocatalyst surface can capture the photoinduced electrons so as to inhibit effectively the recombination of photoinduced electron–hole pairs, which improves the holes to oxidize organic substances. Thus, the increase in the content of adsorbed  $O_2$  can facilitate the separation of photoinduced charge carriers. Moreover, the  $O_2$ –free group, very active to promote the oxidation of organic substances [9], can be formed when the adsorbed  $O_2$  captures photoinduced electrons. Therefore, it could be predicted that the activity of semiconductor photocatalyst would be improved to a certain degree due to the increase in the content of adsorbed  $O_2$  after the noble metal with an appropriate content was deposited, although the step that the adsorbed  $O_2$  captured the photoinduced electrons was very slow so as to greatly influence the photocatalytic reaction [32].

### 3.3. Measurement of SPS

The SPS technique can provide a rapid, non-destructive test of semiconductor solid surface property, and also is a very effective way to study the separation and transfer behavior of photoinduced charge carriers at a surface or interface. The generation of surface photovoltage arises from the creation of electron–hole pairs, followed by the separation under a built-in electric field (the space-charge layer). The difference between the surface potential barrier in the light and that in the dark is the SPS signal [25–28].

Fig. 6 showed the SPS responses of pure and Pd deposited ZnO nanoparticles. It could be found that the SPS peak position of ZnO nanoparticles was at about 360 nm, with the response threshold at 380 nm. In general, the response threshold of bulk ZnO is at 390 nm, indicating that the SPS response of ZnO nanoparticles shifted to the blue, which is attributed to the quantum size effect. According to the energy band structure of ZnO, the strong SPS response could be attributed to the electron transitions from the valence band to conduction band ( $O_{2p} \rightarrow Zn_{3d}$ ) [21]. Moreover, the SPS response of ZnO nanoparticles became much weaker after Pd was deposited. When a noble metal is

Table 1  
The XPS data of  $Zn_{2p}$  and  $O_{1s}$  on the surfaces of pure and Pd deposited ZnO nanoparticles

Samples	Binding energy of three kinds of $O_{1s}$ (eV)	Binding energy of $Zn_{2p}$ (eV)	The atomic number ratio of Zn/O (crystal lattice)	The atomic number ratio of Zn/O (total oxygen)
ZnO	529.9, 531.5, 533.0	1021.9	1.80	0.75
ZnO with Pd	530.3, 531.7, 533.1	1021.7	2.06	0.71

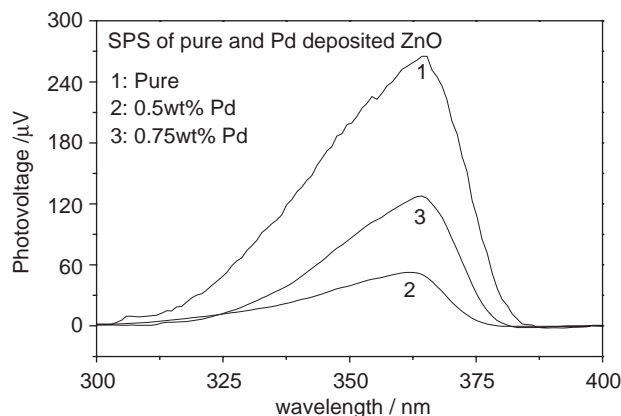


Fig. 6. The SPS responses of pure and Pd deposited ZnO nanoparticles.

contacted with a N-type semiconductor, the Schottky energy barrier at the interface can occur by charge carriers redistributing because the Fermi energy level of the semiconductor is higher than that of the noble metal. This Schottky energy barrier could effectively trap photoinduced electrons, which was responsible for the obvious decrease in the intensity of SPS response of ZnO nanoparticles after the noble metal was deposited on their surfaces [33].

In addition, the effects of the content of deposited Pd on the SPS intensity were very great by influencing the separation efficiency of photoinduced charge carriers. As seen from Fig. 6, the SPS intensity of ZnO nanoparticles with 0.5wt% Pd was weaker than that with 0.75wt% Pd, indicating that the SPS response was weaker if the Pd content was appropriate, otherwise the SPS response would become stronger. This could be explained from the point of the electronic energy level as shown in Fig. 7, selected from the literature [34]. The noble metal Pt deposited  $TiO_2$  was reported in the literature [34]. Moreover, the energy band structure of ZnO is similar to that of  $TiO_2$ . For example, having the nearly same energy level of the conduction band or valence band. Thus, Fig. 7 was listed in the paper to give some explanations about the effects of Pd content on the separation and transfer of photoinduced electron-hole pairs.

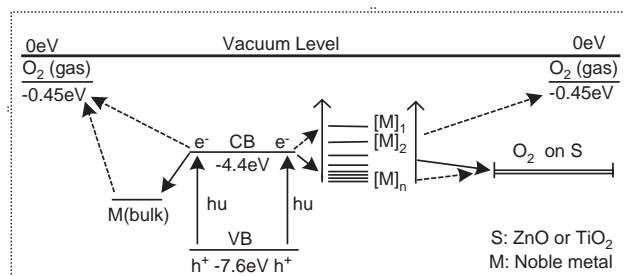


Fig. 7. The electronic energy level of  $O_2$  (gas),  $[M]_n$ , CB,  $O_2$  on S,  $M$  (bulk) and VB.

Fig. 7 showed the electronic energy level of  $O_2$  (gas),  $[M]_n$  (noble metal atomic cluster), conduction band of ZnO or  $TiO_2$  (CB),  $O_2$  on S ( $O_2$  adsorbed on ZnO or  $TiO_2$ ),  $M$  (bulk) and valence band of ZnO or  $TiO_2$  (VB). The electronic energy level of  $[M]_n$  can change to a certain degree with the atomic number of noble metal due to the quantum size effect, namely, the less the atomic number, the higher the electronic energy level, even possibly higher than that of the CB. Thus, the direction of the electrons easily transferring to could be determined according to Fig. 7. The arrowheads of solid line indicated that the electrons could transfer to the direction, while that of dashed line indicated that the electrons could not move to that direction. There were main three results as following: (i) the photoinduced electrons could not transfer directly from the CB to  $O_2$  (gas) or indirectly from the CB to  $O_2$  (gas) via the  $M$  (bulk); (ii) If the electronic energy level of  $[M]_n$  was lower than that of the CB and higher than that of the  $O_2$  (on S) because of the appropriate content of deposited noble metal, the photoinduced electrons could easily transfer indirectly from the CB to  $O_2$  (on S) via the  $[M]_n$  so that the activity of semiconductor photocatalyst was improved by increasing the separation efficiency of photoinduced electron-hole pairs and by promoting the formation of  $O_2$ , meanwhile the semiconductor surface charge changed much smaller, indicating that the SPS response was weak; (iii) If the electronic energy level of  $[M]_n$  was higher than that of the CB because of the very small content of deposited noble metal or was lower than that of the  $O_2$  (on S) because of the very large content of deposited noble metal, the photoinduced

electrons could not transfer indirectly from the CB to  $O_2$  (on S) via the  $[M]_n$  so that the semiconductor surface charge changed to much larger, indicating that the SPS response was strong, and the activity of semiconductor photocatalyst was degraded due to the decrease in the separation efficiency of photoinduced electron–hole pairs.

The above statements indicated that the content of deposited noble metal had great effects on the SPS response and activity of semiconductor photocatalyst, and there were inherent relationships between the SPS response and photocatalytic activity. In other words, the weaker the SPS response, the higher the activity, of noble metal deposited semiconductor photocatalysts.

### 3.4. Measurements of the photocatalytic activity

The photocatalytic activity of ZnO nanoparticles could be evaluated by the photocatalytic oxidation reaction of  $n\text{-C}_7\text{H}_{16}$ . The experiment results showed that the concentration of gas phase  $n\text{-C}_7\text{H}_{16}$  did not change a little after irradiating for 3 h in the absence of the catalyst, indicating that the direct photolysis of  $n\text{-C}_7\text{H}_{16}$  does not take place in our experiment. Fig. 8 showed the evolution curves of gas phase  $n\text{-C}_7\text{H}_{16}$  photocatalyzed on pure 0.5 and 0.75 wt% Pd deposited ZnO nanoparticles, and Fig. 9 reflected the effects of deposited Pd content on the photocatalytic activity of ZnO nanoparticles. It could be seen that the photocatalytic activity of ZnO nanoparticles could be greatly improved after the appropriate content of Pd was deposited on their surfaces. The optimized content of Pd was 0.5 wt%. If the content of deposited Pd was larger than its optimized value, the activity of ZnO nanoparticles began to go down. It should be pointed that the results of photocatalytic activity of ZnO samples were in good agreement with that of XPS and SPS measurements discussed above.

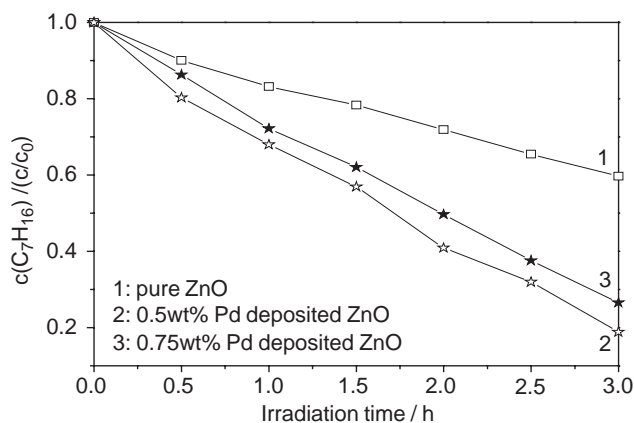


Fig. 8. The evolution curves of gas phase  $n\text{-C}_7\text{H}_{16}$  photocatalyzed on pure and Pd deposited ZnO

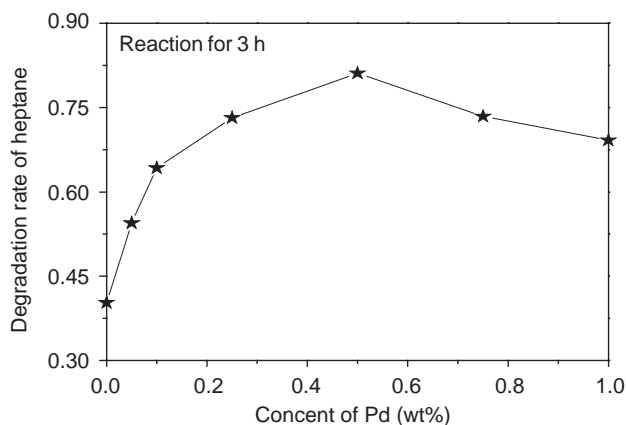


Fig. 9. The effects of deposited Pd content on the photocatalytic activity of ZnO nanoparticles.

## 4. Conclusions

In this paper, the investigations on surface modification of ZnO nanoparticles by depositing noble metal Pd as well as the photocatalytic oxidation reaction of  $n\text{-C}_7\text{H}_{16}$  were carried out, demonstrating that the increase in surface content of adsorbed oxygen was favorable for photocatalytic reaction, and the weaker the SPS response, the higher the photocatalytic activity. Therefore, it could be suggested that the activity of semiconductor photocatalysts would be improved by depositing the noble metal with appropriate content, and its activity could be quickly evaluated by the SPS measurement.

## Acknowledgments

This work was supported by the National Nature Science Foundation of China (Nos. 20171016, 20301006), the Nature Science Foundation of Heilongjiang Province of China (No. B0305), the Science Foundation for Excellent Youth of Heilongjiang Province of China (2002), the supporting plan of Education Bureau of Heilongjiang province (1054G035), the Science Foundation of Chinese Postdoctor (20040350168) and the Science Foundation for Excellent Youth of Heilongjiang University of China (2003).

## References

- [1] L.D. Zhang, J.M. Mou, Nanomaterials and Nanostructure, Science Publisher, Beijing, 2001 P1.
- [2] Y. Murata, S. Fukuta, S. Ishikawa, S. Yokoyama, Sol. Energy Mater. Sol. Cells 62 (2000) 157.
- [3] D.A. Tryk, A. Fujishima, K. Honda, Electrochim. Acta 45 (2000) 2363.

- [4] C.A.K. Gouvêa, F. Wypych, S.G. Moraes, N. Durán, P. Peralta-Zamora, *Chemosphere* 40 (2000) 427.
- [5] X. Qian, X. Zhang, Y. Bai, T. Li, X. Tang, E. Wang, S. Dong, *J. Nanoparticle Res.* 2 (2000) 191.
- [6] E.R. Carraway, A.J. Hoffman, M.R. Hoffmann, *Environ. Sci. Technol.* 28 (1994) 786.
- [7] I.L. Marta, *Appl. Catal. B* 23 (1999) 89.
- [8] A. Fujishima, T.N. Rao, D.A. Tryk, *J. Photochem. Photobiol. C* 1 (2000) 1.
- [9] M.R. Hoffmann, S.T. Martin, W. Choi, D.W. Bahnemann, *Chem. Rev.* 95 (1995) 69.
- [10] A. Fujishima, T.N. Rao, *Pure Appl. Chem.* 70 (1998) 2177.
- [11] A.L. Linsebigler, G.Q. Lu, J.T. Yates, *Chem. Rev.* 95 (1995) 735.
- [12] K. Sunada, Y. Kikuchi, K. Hashimoto, A. Fujishima, *Environ. Sci. Technol.* 32 (1998) 726.
- [13] B. Ohtani, K. Iwai, S. Nishimoto, S. Sato, *J. Phys. Chem. B* 101 (1997) 3349.
- [14] A. Sclafani, J.M. Herrmann, *J. Photochem. Photobiol. A* 113 (1998) 181.
- [15] J. Papp, H.S. Shen, R. Kershaw, K. Dwight, A. Wold, A. Wold, *Chem. Mater.* 5 (1993) 284.
- [16] S. Cheng, U. Nickel, *Chem. Commun.* 2 (1998) 133.
- [17] J.M. Herrmann, H. Tahiri, Y. Ait-Ichou, G. Lassaletta, A.R. González-Elipé, A. Fernández, *Appl. Catal. B* 13 (1997) 219.
- [18] X.Z. Li, F.B. Li, *Environ. Sci. Technol.* 35 (2001) 2381.
- [19] A. Blažková, I. Csölleová, V. Brezová, *J. Photochem. Photobiol. A* 113 (1998) 251.
- [20] Y. Hao, M. Yang, W. Li, X. Qiao, L. Zhang, S. Cai, *Sol. Energy Mater. Sol. Cells* 60 (2000) 349.
- [21] L.Q. Jing, Z.L. Xu, X.J. Sun, J. Shang, W.M. Cai, *Appl. Surf. Sci.* 180 (2001) 308.
- [22] L.Q. Jing, Y.G. Zheng, Z.L. Xu, D.F. Zheng, F.X. Dong, *Chem. J. Chin. Univ.* 22 (2001) 1885.
- [23] L.Q. Jing, X.J. Sun, Z.L. Xu, J. Shang, W.M. Cai, *Acta Chim. Sin.* 60 (2002) 1778.
- [24] L.Q. Jing, W.M. Cai, X.J. Sun, Z.L. Xu, *Chin. J. Catal.* 23 (2002) 336.
- [25] Y.H. Lin, D.J. Wang, Q.D. Zhao, M. Yang, Q.L. Zhang, *J. Phys. Chem. B* 108 (2004) 3202.
- [26] L. Kronik, Y. Shapira, *Surf. Sci. Rep.* 37 (1999) 1.
- [27] D. Wang, Y. Cao, X. Zhang, Z. Liu, X. Qian, X. Ai, F. Liu, D. Wang, Y. Bai, T. Li, X. Tang, *Chem. Mater.* 11 (1999) 392.
- [28] X. Qian, D. Qin, Q. Song, Y. Bai, T. Li, X. Tang, E. Wang, S. Dong, *Thin Solid Films* 385 (2001) 152.
- [29] J. Shang, Y.G. Du, Z.L. Xu, *Chemosphere* 46 (2002) 93.
- [30] L.Q. Jing, Z.L. Xu, Y.G. Du, X.J. Sun, W.M. Cai, *Chem. J. Chin. Univ.* 23 (2002) 871.
- [31] X.Z. Cao, W.H. Zhang, T.Y. Song, *Inorganic Chemistry*, Higher Education Publisher, Beijing, 1991, p.150.
- [32] H. Gerisher, A. Heller, *J. Phys. Chem.* 95 (1991) 5261.
- [33] L.Q. Jing, Z.L. Xu, J. Shang, X.J. Sun, W.M. Cai, H.G. Fu, *Sol. Energy Mater. Sol. Cell* 79 (2003) 133.
- [34] M. Sadeghi, W. Liu, T.G. Zhang, P. Stavropoulos, B. Levy, *J. Phys. Chem.* 100 (1996) 19466.